Controlled, Stepwise Reduction and Band Gap Manipulation of Graphene Oxide

ARTICLE *in* JOURNAL OF PHYSICAL CHEMISTRY LETTERS · APRIL 2012

Impact Factor: 7.46 · DOI: 10.1021/jz300096t

8 AUTHORS, INCLUDING:

Charudatta Galande
Rice University
30 PUBLICATIONS **505** CITATIONS
SEE PROFILE

Kaushik Balakrishnan
The University of Arizona
36 PUBLICATIONS **1,987** CITATIONS
SEE PROFILE

Leela Mohana Reddy Arava
Wayne State University
72 PUBLICATIONS **3,974** CITATIONS
SEE PROFILE

THE JOURNAL OF PHYSICAL CHEMISTRY Letters

Letter

pubs.acs.org/JPCL

Controlled, Stepwise Reduction and Band Gap Manipulation of Graphene Oxide

Akshay Mathkar,[†] Dylan Tozier,[‡] Paris Cox,[†] Peijie Ong,[§] Charudatta Galande,[†] Kaushik Balakrishnan,[†] Arava Leela Mohana Reddy,[†] and Pulickel M. Ajayan*[,†]

[†]Department of Mechanical Engineering & Materials Science, Rice University, Houston, Texas 77005, United States

[‡]Department of Chemical and Biomolecular Engineering, Rice University, Houston, Texas 77005, United States

[§]Department of Materials Science & Engineering, Cornell University, Ithaca, New York 14583, United States

Supporting Information

ABSTRACT: Graphene oxide (GO) has drawn tremendous interest as a tunable precursor in numerous areas, due to its readily manipulable surface. However, its inhomogeneous and nonstoichiometric structure makes achieving chemical control a major challenge. Here, we present a room-temperature based, controlled method for the stepwise reduction of GO, with evidence of sequential removal of each organic moiety. By analyzing signature infrared absorption frequencies, we identify the carbonyl group as the first to be reduced, while the tertiary alcohol takes the longest to be completely removed from the GO surface. Controlled reduction allows for progressive tuning of the optical gap from 3.5 eV down to 1 eV, while XPS spectra show a concurrent increase in the C/O ratio. This study is the first step toward selectively enhancing the chemical homogeneity of GO, thus providing greater control over its structure, and elucidating the order of removal of functional groups and hydrazine-vapor reduction.

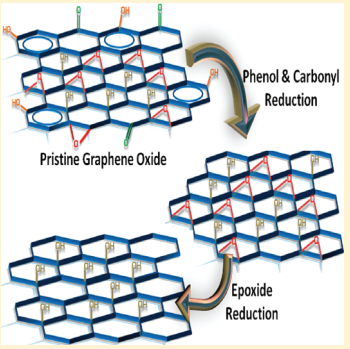

SECTION: Physical Processes in Nanomaterialsand Nanostructures

Due to its exceptional electronic,[1,2] mechanical,[3] and optical properties[1−4] and its potential for applications, graphene[1−3] and methods for its synthesis have garnered a lot of attention in recent times. A widely adopted approach that has shown great promise is the chemical reduction of graphite oxide, and, as a result, gaining insights into the heterogeneous structure of graphene oxide (GO) has been the focus of numerous studies.[5−9] GO is a complex chemical system consisting of a graphene sheet covalently bonded to oxygen-bearing groups, with epoxy and hydroxyl functional groups occupying the basal plane, and carbonyl, carboxylic acid, and lactol functionalities attached to the edges.[10] The presence of these moieties results in a disruptive sp^3 hybridized network and a reduced number of conductive pathways, giving GO its insulating characteristics. Conventional methods that are employed to efficiently reduce GO include, but are not restricted to, reaction with $NaBH_4$,[10] hydrazine,[11] and thermal annealing, yielding its conductive counterpart, reduced graphene oxide[12,13] (RGO). Recently, however, the focus has shifted to GO itself, particularly in terms of the structural transitions in its sp^2/sp^3 fraction and achieving control over its chemical characteristics as it is reduced. Among these studies, Bagri et al.[14] have reported significant insights into the reduction of GO upon thermal annealing based on molecular dynamics simulations. Other studies that attempt to manipulate the C/O ratios of chemically modified graphenes (CMGs) involve annealing at temperatures greater than 150 °C or the use of specific polar organic solvents[15] with no evidence of chemical selectivity or control over organic functionalities on the surface of GO. Heating at higher temperatures results in pyrolysis of organic moieties,[5] making it tedious to extract explicit information about individual functionalities, thus calling for a facile method at less harsh reaction conditions.

Herein we present a protocol for reduction of GO using a gas-based hydrazine reduction method with specific control over each organic moiety, resulting in stepwise removal of functional groups and, for the first time, elucidating the *order* of reduction of each functional group from the surface of GO. Free standing graphite oxide membranes (see Experimental Methods) were reduced by exposure to hydrazine vapors at times ranging from 30 min to 1 week. Attenuated total reflection/Fourier transform infrared (ATR-FTIR) measurements on each of the partially reduced graphene oxide (pRGO) films show sequential removal of functional groups from GO, with a direct correlation to the time of exposure to hydrazine vapor, i.e., the extent of reduction. Having the ability to control the functional groups on GO in a micrometer-thick free-standing film allows for direct solution processing. In addition to forming stable suspensions in polar organic solvents, stepwise reduction results in remnant groups on the graphene surface that contribute to electrostatic repulsion,[16] giving it the unique ability to produce stable suspensions in water without

Received: January 24, 2012
Accepted: March 27, 2012

   dx.doi.org/10.1021/jz300096t | *J. Phys. Chem. Lett.* 2012, 3, 986−991

surfactants (see Supporting Information, Figure S2). Existing reduction methods involve extremely fast kinetics, making it difficult to experimentally gauge the chemical behavior of each organic moiety during reduction. On the other hand, the relatively mild chemical nature of hydrazine vapors, as well as the ability to carry out the reduction of GO at room temperature, results in a slower rate of reduction, thus permitting comprehensive characterization and understanding of the removed/remnant functional groups using a combination of ATR-FTIR, UV−visible (UV−vis) spectroscopy and X-ray photoelectron spectroscopy (XPS).

ATR-FTIR of a free-standing film of GO within 800−2000 cm^{-1} accounts for the characteristic functionalities that are present on the surface of a sheet of GO (Figure 1b). While

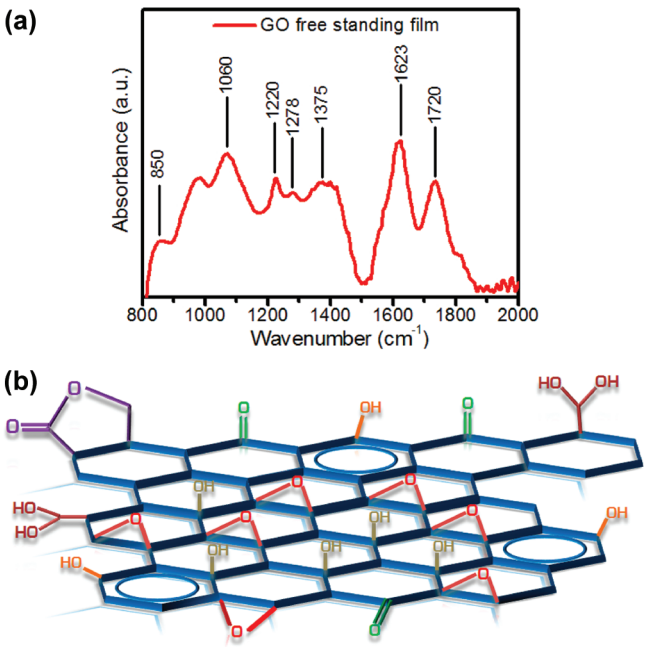

Figure 1. (a) ATR-FTIR spectrum of a free-standing film of GO. Focusing on the characteristic region of the FTIR spectrum reveals clear peaks at 1720 cm^{-1}, 1220 cm^{-1} (epoxide stretch), 850 cm^{-1} (epoxide bend), 1060 cm^{-1} (alkoxy), 1375 cm^{-1} (tertiary alcohol), and 1278 cm^{-1} (phenol). (b) A structural model of GO. All the functional groups that are present in the FTIR spectrum are accounted for, specifically, carbonyl (green), epoxide (red), tertiary alcohols (gray), and phenols (orange).[10] The hydrophilic nature of GO leads to noncovalent intercalation of moisture between sheets[5].

hydroxyl (−OH) groups *do* have a prominent absorption band between 3000 and 3500 cm^{-1} (see Supporting Information, Figure S5), a large contribution due to the presence of moisture intercalated within hydrophilic GO sheets makes it difficult to resolve the alcoholic functionalities within this region. Thus, as shown in Figure 1a, we focus on specific peaks within the 800−2000 cm^{-1} region.[17] The peaks at 850 cm^{-1} and 1220 cm^{-1} represent the bending and asymmetric stretching modes of the epoxy (C−O−C) group, while the peak at 1060 cm^{-1} is characteristic of alkoxy (C−O) vibrations. The peak at 1278 cm^{-1} corresponds to phenolic groups (Ar−OH), while the broad series of peaks that follows between 1300−1450 cm^{-1} consist of a peak embedded at ∼1375 cm^{-1} corresponding to tertiary alcohol bending.[20,21] In Figure 1a, this peak is embedded within an even stronger feature at ∼1420 cm^{-1} corresponding to aryl (C═C) stretching, but upon reduction, its presence in subsequently partially reduced spectra becomes evident. The intense peak at 1620 cm^{-1} is attributed to the bending mode of water molecules. Lastly, the peak at 1720 cm^{-1} represents the stretching mode of carbonyl (C═O) bonds in both ketone and carboxylic acid groups.[20]

Upon exposure to hydrazine vapors, noticeable changes in the FTIR spectra were observed at exposure times starting at 150 min (2.5 h). Figure 2a (i) shows absorbance spectra of free-standing films of GO and pRGO at reduction times of 2.5 h, 4 h, and 8 h. The color of the brown GO membrane became noticeably darker within the first 2 h, but the pRGO retained the hydrophilic nature of GO, forming stable suspensions in water upon ultrasonication, at concentrations up to 1 mg/mL, until 8 h of hydrazine exposure . After 2.5 h, the FTIR spectrum showed an unambiguous drop in the intensity of the C═O peak at 1720 cm^{-1}, and a progressive, continuous decrease was noted until the peak was completely eliminated at 8 h. Identical reduction patterns were exhibited by the phenol (Ar−OH) peak, initially present as a well-resolved peak at 1278 cm^{-1}, and its intensity decreased significantly after hydrazine exposure for 2.5 h (Figure 2a,ii). Subsequent spectra showed a progressively weakening feature, and complete reduction was apparent at 16 h.

The epoxide peak(s) also showed similar trends, albeit at different exposure times. Of the two characteristic epoxy peaks, the asymmetric stretch peak at 1220 cm^{-1} (Figure 2b,i) was the first to decrease in intensity and could not be detected after 4 h of hydrazine exposure. The epoxide bending peak present at 850 cm^{-1} (Figure 2b,ii), however, was still observed, indicating that epoxy groups were still present. This peak continued to decrease in intensity until 21.5 h, after which it could not be detected. Both of these peaks were absent in all subsequent spectra, indicating complete elimination of epoxide moieties upon 21.5 h of hydrazine exposure. The progression of the tertiary alcohol peak is shown in Figure 2a,iii, where the spectrum of GO shows a broad feature between 1300 and 1450 cm^{-1}, consisting of several closely spaced peaks representing multiple bonds, as described earlier. After exposure to hydrazine vapors, a significant change in the line shape of the broad feature was observed at 8 h, indicating a decrease in spectral weight of a peak embedded within the band. Tertiary alcohol groups are known to absorb at around ∼1375 cm^{-1} in the bonded state (OH deformation), which is exactly the region where the decrease in spectral weight is observed. The absorption intensity at 1375 cm^{-1} progressively decreases up to 108 h, until only a well-resolved band is observed at 1420 cm^{-1}, which can be attributed to the stretching mode of aryl (C═C) bonds. We conclude that tertiary alcohol groups undergo near-complete removal up to 108 h. Previous studies have raised concerns regarding the difficulty in reduction of hydroxyl groups, including the possibility of it not being reduced at all.[5] Our data indicates that it is only after extended exposure to hydrazine vapors that the alcohol groups are reduced, and the removal occurs much later than all the other functional groups; this difficulty in reduction may be attributed to steric hindrance slowing down the reaction process. The trends observed in our data show carbonyl groups to be most reactive, being the first to be reduced at 8 h. Phenolic and epoxy groups are then reduced at 16 and 21.5 h, respectively, while tertiary alcohols are reduced only after 108 h of exposure.

Another key area of investigation within hydrazine-based reduction is the incorporation of nitrogen-based organic groups on the surface of GO. Previous studies have illustrated the

dx.doi.org/10.1021/jz300096t | J. Phys. Chem. Lett. 2012, 3, 986−991

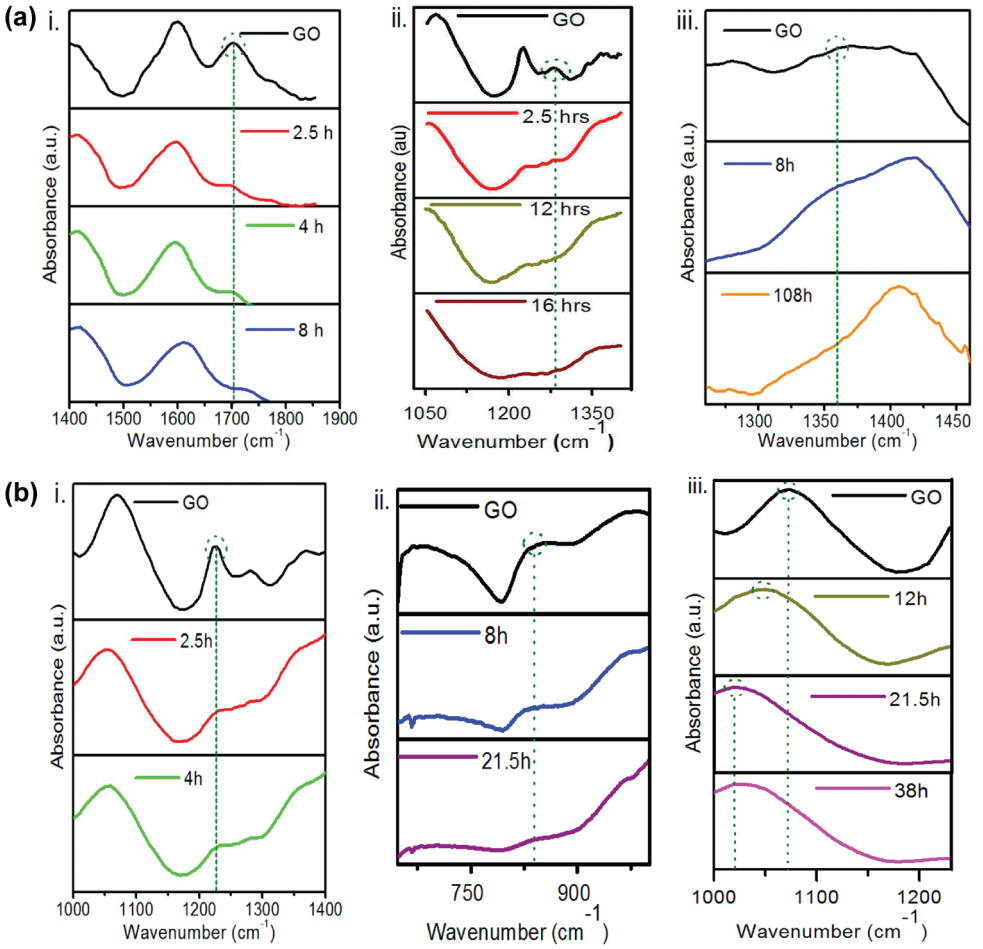

Figure 2. (a) Reduction of carbonyl, phenol, and tertiary alcohol moieties at different times of hydrazine exposure. IR spectra reveal sequential reduction of (i) carbonyl (1720 cm^{-1}), (ii) phenol (1278 cm^{-1}), and (iii) tertiary alcohol (1375 cm^{-1}) functional groups. The carbonyl group is completely reduced after 8 h, after which the phenol moiety is removed at 16 h, and finally the tertiary alcohol at 108 h of hydrazine vapor exposure. (b) Reduction of the epoxide group and a shift in the alkoxy peak. Evidence of sequential reduction of the epoxide group is noted due to a decrease in the intensity of (i) molecular stretching (1220 cm^{-1}) and (ii) bond bending (850 cm^{-1}), leading to the conclusion that complete reduction occurs after 21.5 h. The alkoxy peak (iii) is seen to progressively shift from 1060 cm^{-1} to 1020 cm^{-1}, serving as a possible indicator for nitrogen-substitution at alkoxy sites.

significance of edges in graphene,[22] particularly during N-substitution in graphene,[23] and a number of current studies are focused on identifying the explicit chemical composition of the resulting organic moieties and the respective reaction mechanisms. Our data sheds new light on these claims, specifically in terms of the site of reaction: the absorption peak at 1060 cm^{-1}, which accounts for the presence of alkoxy moieties (C−O) bonds, showed no change after initial exposure to hydrazine. However after 12 h, a slight shift in the peak position was noted, and this progressive downshift continued to 1020 cm^{-1} at 38 h (Figure 2b,iii). Peaks in this region correspond to either in-plane aromatic vibrations or C−N moieties.[20] The C/N ratio was seen to decrease upon hydrazine exposure, from 200:1 down to 22:1 after 12 h, implying substitution of nitrogen-based moieties on the GO surface, quite possibly with a reaction initiating from the alkoxy bond. Our findings compare differently to other studies[19] that employ more severe reduction treatments, implying completely separate mechanisms for each method of reduction.

Understanding the electronic band structure of GO has been complicated due to its large structural and chemical inhomogeneity. Yet, both theoretical and experiment evidence suggests the presence of an energy gap in GO and its direct dependence on the fraction of sp^2/sp^3 hybridized domains.[24] Jeong and co-workers[25,26] showed a systematic transition in the optical gap by varying the oxidation time during Hummer's method. However, given the extremely rapid kinetics of oxidation, it is difficult to suggest a particular instance (i.e., point of time) at which the introduction of a certain functional group occurs, making it virtually impossible to achieve any degree of control over the chemical composition. As a consequence, the influence that each of the functional groups has on the optical gap is unclear. The mild nature of hydrazine vapors allows us to smoothly tailor the optical gap of insulating GO and probe its dependence on various functional groups during reduction. With the results we have obtained, approaching the problem by identifying the instance of the *removal* of each functional group and its corresponding consequence on the band gap makes it more feasible to extend this analysis to similar studies that attempt controlled manipulation of GO, instead of varying the oxidation conditions.

dx.doi.org/10.1021/jz300096t | *J. Phys. Chem. Lett.* 2012, 3, 986−991

The energy gap was calculated from UV−vis absorption spectra using the following form of Tauc's expression:[27,28]

$$\omega^2\varepsilon = (h\omega - E_g)^2 \quad (1)$$

where ε is the absorption intensity, ω $(2\pi/\lambda)$ is the angular frequency of the incident radiation, and E_g is the optical band gap. As shown in previous reports,[29,30] plotting $\varepsilon^{1/2}/\lambda$ against the energy (hc/λ) and extrapolating the linear region of the curve to the x-axis gives the optical band gap. Figure 3

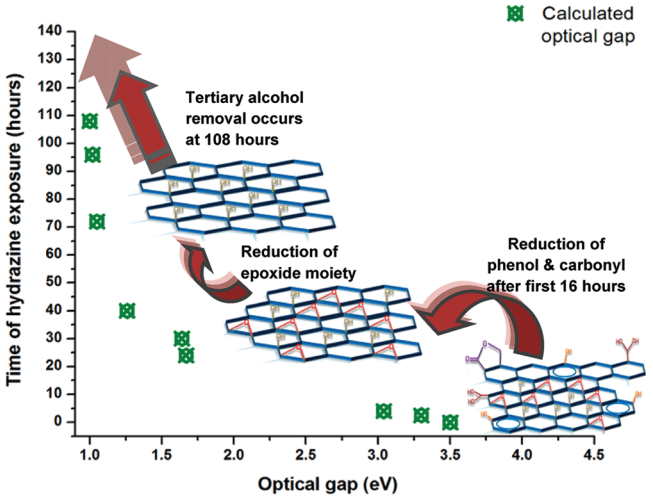

Figure 3. Gradual decrease in optical band gap upon exposure to hydrazine vapors accompanied by a schematic of the approximate pRGO structure at that point of time. The optical gap, as calculated by Tauc's analysis (see Supporting Information, Figure S4A−C) shows a progression from 3.5 eV down to 1 eV. By correlating the time of removal of each functional group (see Figure 2), the approximate structures of pRGO are sketched.

summarizes the variation in optical gap (E_g) during hydrazine-vapor reduction, with the approximate structures of pRGO. Within the first 8 h, a significant reduction is seen in the optical energy gap. Initially, the insulating characteristics of GO are well represented (3.5 eV, 0 h), but upon continuous exposure for 4 h, the E_g progressively decreases to 3.3 eV (2.5 h) and then 3.0 eV (4 h). Over the next 30 h, a sharp decrease is seen in E_g, which is in conjunction with the FTIR results that show a majority of the moieties being reduced during the same time frame. Upon removal of phenolic and epoxy moieties, the optical energy gap is seen to progress toward values that are generally less characteristic of insulators, and closer to those of semiconductors (~1.6 eV, 30 h), which has not been achieved with GO to our knowledge. The drastic reduction in band gap, which is evident up to approximately 45 h, slows down after this point, providing a qualitative idea of the difficulty associated with the removal of the tertiary alcohol. Upon complete removal (>108 h), the band gap shows an elegant progression down to 1 eV, and remains at this value when reduced upon further hydrazine exposure.

Isolating the relative abundance of the functional groups requires intricate and time-consuming analytical techniques,[10,18,31] but would provide a lot more useful information regarding the structure and mechanism of reduction, and is an avenue for future studies. From the evidence noted, the hypothesis that each functional group plays a key role in the decrease in optical gap is well represented. XPS spectra of each pRGO mirrored a similar sequential increase in C/O atomic ratio at the times of functional group removal as seen in Figure 4, reflecting the results shown by both FTIR and band gap data.

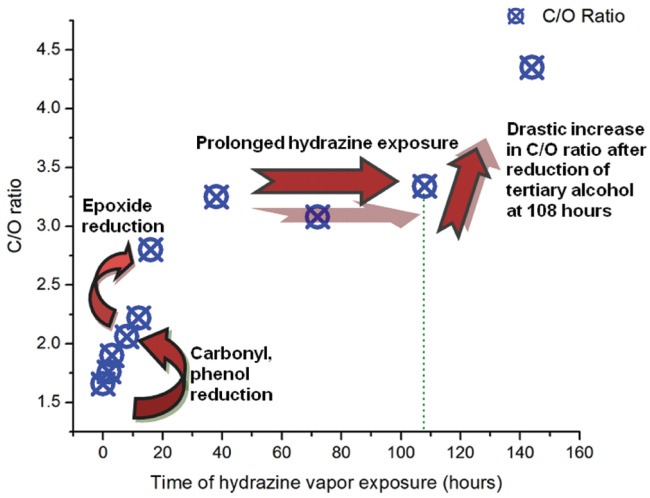

Figure 4. Increasing C/O ratio of free-standing pRGO films upon exposure to hydrazine vapors. Progression is observed from a ratio of ~1.7 in pristine GO to spikes in the C/O ratio at precisely the same points of removal of each organic moiety. The final C/O ratio of ~4.5 is considerably less than that of conventional RGO, which is why the optical band gap does not decrease below 1 eV when reduced by hydrazine vapors.

First, there is a notable spike from 8 to 16 h, which is exactly when the carbonyl moiety is reduced (Figure 2a,i). Second, the initial increase in the C/O ratio is a lot greater than that after ~40 h, indicating that the majority of reduction has occurred up to that point, which also is supported by both FTIR spectra and the consequent decrease in E_g. The C/O ratio is approximately 4.5 upon removal of the identified moieties, which is a lot less than the values obtained by stronger modes of treatment. Pinpointing a reason for the difficulty of removal of a *particular* functional group is a complex problem since it depends on the progression of reduction and the chemical reactions of hydrazine vapors with each functional group. On the other hand, we have been able to identify the functional group associated with the transition into each regime by correlating it with the degree of reduction and the optical band gaps. It is important to realize that hydrazine vapors were chosen as a candidate for reduction due to their mild nature of reduction, which is why lower optical band gaps (<0.9 eV) and higher C/O ratios were not observed. To ensure this, a Tauc plot was also made for CCG1, which showed an optical band gap of 0.85 eV (Supporting Information, Figure S4C), indicating a degree of reduction much greater than the partially reduced samples we report. The optical gap of 1 eV was noted as a limit of the hydrazine vapor method, as upon further exposure it was not seen to decrease further. Reasons for this include the presence of incompletely reduced oxygen groups as has been noted previously by Robinson and co-workers[32] due to the weak penetrative nature of hydrazine vapors, as well as structural defects in RGO films.[33]

In summary, we have presented a room-temperature-based reduction method for GO using hydrazine vapors to illustrate evidence of controlled removal of chemical functionalities from its surface. ATR-FTIR spectroscopy was successfully applied to probe the stepwise removal of functional groups at different

dx.doi.org/10.1021/jz300096t | J. Phys. Chem. Lett. 2012, 3, 986−991

stages of reduction. The sequential removal of each moiety as GO evolves through its partially reduced states is confirmed by a progressive decrease in its optical energy gap from 3.5 eV down to 1 eV, and XPS spectra show a corresponding increase in the C/O ratios at the exact intervals of times in which we identify a particular functional group to be eliminated. A decrease in the C/N ratio over time also suggests nitrogen-doping due to hydrazine vapors, with the possibility of chemical substitution at the alkoxy group sites. Our method of reduction allows us to isolate stable, free-standing films of pRGO, at any stage of reduction, which opens possibilities for controlling the chemical composition of graphene-like materials, and tuning its optical and electronic properties for a broad range of applications.[34−36]

EXPERIMENTAL METHODS

Synthesis of GO. Graphite powder (45 μm, >99.99 wt %, Aldrich) was used as a starting material. GO was synthesized by the improved Hummer's method[31] and purified accordingly, to yield a brown powder, which was readily dispersed in deionized (DI) water to produce a stable suspension. No settling was observed over 2 weeks.

Preparation of Free-Standing Films. Free standing GO films were prepared by vacuum filtration through a 25 nm pore mixed cellulose ester membrane (Millipore) followed by overnight drying in a vacuum desiccator. The resulting membrane was readily peeled off the filter paper, to yield a flexible free-standing film of GO.

Reduction of GO. Twenty-five milliliters of hydrazine hydrate (Sigma Aldrich) was placed in an open 50 mL beaker in a vacuum desiccator (in-house vacuum, 100 mTorr). The free-standing film was cut into equal pieces (55 ± 2 mg) and reduced at times ranging from 30 min to 7 days by exposure to hydrazine vapors under vacuum at room temperature to yield pRGO films. Each piece was individually reduced, and upon removal from the desiccator, not subject to further reduction (i.e., hydrazine vapor exposure). Upon reduction, the brown GO was seen to slowly alter to black pRGO films. Free-standing films allow for equal exposure of the surface of GO sheets to hydrazine vapors, resulting in even reduction of GO sheets. In comparison, GO powders result in incomplete reduction, as the top layer was observed to be black, but the remaining powder retained the brown color of GO. CCG1 was synthesized as described elsewhere, and the solid product was isolated by vacuum filtration.

Characterization. FTIR analysis was done on a Nicolet FTIR microscope with a MCT/A detector in the ATR mode. For UV−vis absorption measurements, GO (250 mg/L) was suspended in DI water, whereas pRGO samples were dispersed in DI water using sodium dodecyl sulfate. Absorption measurements were done on a Shimadzu 3600 UV−vis spectrophotometer. XPS analysis was done on a PHI Quantera X-ray photoluminescence spectrometer, at a chamber pressure of 5×10^{-9} Torr and with an Al cathode as the X-ray source, with power set to 100 W. The pass energy for the survey scan was 140.00 eV.

ASSOCIATED CONTENT

Supporting Information

Specifics of hydrazine-vapor reduction procedure, UV−vis absorption, Tauc plots at different times of hydrazine-vapor exposure, and images confirming the stability of free-standing films in solution. This material is available free of charge via the Internet at http://pubs.acs.org

AUTHOR INFORMATION

Corresponding Author

*E-mail: ajayan@rice.edu.

Notes

The authors declare no competing financial interest.

ACKNOWLEDGMENTS

A.M. would like to thank A. Mohite and W. Gao for helpful discussions.

REFERENCES

(1) Green, A. A.; Hersam, M. C. Solution Phase Production of Graphene with Controlled Thickness via Density Differentiation. *Nano Lett.* **2009**, *9*, 4031−4036.

(2) Terrones, M.; Botello-Mendez., A. R.; Campos-Delgado, J.; Lopez-Urias, F.; Vega-Cantu, Y. I.; Rodriguez-Macias, F. J.; Elias, A. L.; Munoz-Sandoval, E.; Cano-Marquez, A. G.; Charlier, J.; et al. Graphene and Graphite Nanoribbons: Morphology, Properties, Synthesis, Defects and Applications. *Nano Today* **2010**, *5*, 351−372.

(3) Tung, V. C.; Allen, M. J.; Yang, Y.; Kaner, R. B. High-Throughput Solution Processing of Large-Scale Graphene. *Nat. Nanotechnol.* **2009**, *4*, 25−29.

(4) Wassei, J. K.; Kaner, R. B. Graphene, a Promising Transparent Conductor. *Mater. Today* **2010**, *13*, 52.

(5) Stankovich, S.; Dikin, D. A.; Piner, R. D.; Kohlhaas, K. A.; Kleinhammes, A.; Jia, Y.; Wu, Y.; Nguyen, S. T.; Ruoff, R. S. Synthesis of Graphene-Based Nanosheets via Chemical Reduction of Exfoliated Graphite Oxide. *Carbon* **2007**, *45*, 1558−1565.

(6) Gilje, S.; Han, S.; Wang, M.; Wang, K. L.; Kaner, R. B. A Chemical Route to Graphene for Device Applications. *Nano Lett.* **2007**, *7*, 3394−3398.

(7) Eda, G.; Fanchini, G.; Chhowalla, M. Large-Area Ultrathin Films of Reduced Graphene Oxide as a Transparent and Flexible Electronic Material. *Nat. Nanotechnol.* **2008**, *3*, 270.

(8) Lerf, A.; He, H. Y.; Forster, M.; Klinowski, J. Structure of Graphite Oxide Revisited. *J. Phys. Chem. B* **1998**, *102*, 4477−4482.

(9) He, H. Y.; Klinowski, J.; Forster, M.; Lerf, A. A New Structural Model for Graphite Oxide. *Chem. Phys. Lett.* **1998**, *287*, 53.

(10) Gao, W.; Alemany, L.; Ci, L.; Ajayan, P. New Insights into the Structure and Reduction of Graphite Oxide. *Nat. Chem.* **2009**, *1*, 403−408.

(11) Wang, Y.; Shi, Z.; Huang, Yi.; Ma, Y.; Wang, C.; Chen, M.; Chen, Y. Supercapacitor Devices Based on Graphene Materials. *J. Phys. Chem. C* **2009**, *113*, 13103−1310.

(12) Gilje, S.; Dubin, S.; Badakhshan, A.; Farrar, J.; Danczyk, S. A.; Kaner, R. B. Photothermal Deoxygenation of Graphene Oxide for Patterning and Distributed Ignition Applications. *Adv. Mater.* **2010**, *22*, 419−423.

(13) Stoller, M. D.; Park, S. J.; Zhu, Y. W.; An, J. H.; Ruoff, R. S. Graphene-Based Ultracapacitors. *Nano Lett.* **2008**, *8*, 3498−3502.

(14) Bagri, A.; Mattevi, C.; Acik, M.; Chabal, Y. J.; Chhowalla, M.; Shenoy, V. B. Structural Evolution During the Reduction of Chemically Derived Graphene Oxide. *Nat. Chem.* **2010**, *2*, 581−587.

(15) Compton, O. C.; Jain, B.; Dikin, D. A.; Abouimrane, A.; Amine, K; Nguyen, S. T. Chemically Active Reduced Graphene Oxide with Tunable C/O Ratios. *ACS Nano* **2011**, *5*, 4380.

(16) Li, D.; Muller, M. B.; Gilje, S.; Kaner, R. B.; Wallace, G. G. Processable Aqueous Dispersions of Graphene Nanosheets. *Nat. Nanotechnol.* **2008**, *3*, 101−105.

(17) Si, Y.; Samulski, E. T. Synthesis of Water Soluble Graphene. *Nano Lett.* **2008**, *8*, 1679−1682.

(18) Acik, M.; Lee, G.; Mattevi, C.; Chhowalla, M.; Cho, K.; Chabal, Y. J. The Role of Oxygen during Thermal Reduction of Graphene

Oxide Studied by Infrared Absorption Spectroscopy. *Nat. Mater.* **2010**, *9*, 840−845.
(19) Gao, X.; Jang, J.; Nagase, H. Hydrazine and Thermal Reduction of Graphene Oxide: Reaction Mechanisms, Product Structures, and Reaction Design. *J. Phys. Chem. C* **2010**, *114*, 832−842.
(20) Colthup, N. B.; Daly, L. H.; Wiberley, S. E. *Introduction to Infrared and Raman Spectroscopy*, 3rd ed.; Academic Press: London; 1990.
(21) Collins, W. R.; Schmois, E.; Swager, T. M. Graphene Oxide as an Electrophile for Carbon Nucleophiles. *Chem. Commun.* **2011**, *47*, 8790−8792.
(22) Jia, X.; Campos-Delgado, J.; Terrones, M.; Meunier, V.; Dresselhaus, M. S. Graphene Edges: A Review of Their Fabrication and Characterization. *Nanoscale* **2011**, *3*, 86.
(23) Wang, X.; Li, X.; Zhang, L.; Yoon, Y.; Weber, P. K.; Wang, H.; Guo, J.; Dai, H. N-Doping of Graphene through Electrothermal Reactions with Ammonia. *Science* **2009**, *324*, 768−771.
(24) Eda, G.; Mattevi, C.; Yamaguchi, H.; Kim, H.; Chhowalla, M. Insulator to Semimetal Transition in Graphene Oxide. *J. Phys. Chem. C* **2009**, *113*, 15768−15771.
(25) Jeong, H. K.; Jin, M. H.; So, K. P.; Lim, S. C.; Lee, Y. H. Tailoring the Characteristics of Graphite Oxides by Different Oxidation Times. *J. Phys. D: Appl. Phys.* **2009**, *42* (065418), 1−6.
(26) Jin, M.; Jeong, H. K.; Yu, W. J.; Bae, D. J.; Kang, B. R.; Lee, Y. H. Graphene Oxide Thin Film Field Effect Transistors without Reduction. *J. Phys. D: Appl. Phys.* **2009**, *42* (135109), 1−5.
(27) Tauc, J. Optical Properties and Electronic Structure of Amorphous Ge and Si. *Mater. Res. Bull.* **1968**, *3*, 37−46.
(28) Tauc, J.; Grigorovici, R.; Vancu, A. Optical Properties and Electronic Structure of Amorphous Germanium. *Phys. Status Solidi* **1996**, *15*, 627−637.
(29) Ci, L.; Song, L.; Jin, C.; Jariwala, D.; Wu, D.; Li, Y.; Srivastava, A.; Wang, Z. F.; Storr, K.; Balicas, L.; et al. Atomic Layers of Hybridized Boron Nitride and Graphene Domains. *Nat. Mater.* **2010**, *9*, 430−435.
(30) Song, L.; Ci, L.; Lu, H.; Sorokin, P. B.; Jin, C.; Ni, J.; Kvashnin, A. G.; Kvashnin, D. G.; Lou, J.; Yakobson, B. I.; et al. Large-Scale Growth and Characterization of Atomic Hexagonal Boron Nitride Layers. *Nano Lett.* **2010**, *10*, 3209−3215.
(31) Marcano, D. C.; Kosynkin, D. V.; Berlin, J. M.; Sinitskii, A.; Sun, Z.; Slesarev, A.; Alemany, L. B.; Lu, W.; Tour, J. M. Improved Synthesis of Graphene Oxide. *ACS Nano* **2010**, *4*, 4806−4814.
(32) Robinson, J. T.; Perkins, F. K.; Snow, E. S.; Wei, Z.; Sheehan, P. E. Reduced Graphene Oxide Molecular Sensors. *Nano Lett.* **2008**, *8*, 3137−3140.
(33) Gómez-Navarro, C.; Meyer, J. C.; Sundaram, R. S.; Chuvilin, A.; Kurasch, S.; Burghard, M.; Kern, K.; Kaiser, U. Atomic Structure of Reduced Graphene Oxide. *Nano Lett.* **2010**, *10*, 1144−1148.
(34) Murray, I. P.; Lou, S. J.; Cote, L. J.; Loser, S.; Kadleck, C. J.; Xu, T.; Szarko, J. M.; Rolczynski, B. S.; Johns, J. E.; Huang, J.; et al. Graphene Oxide Interlayers for Robust, High-Efficiency Organic Photovoltaics. *J. Phys. Chem. Lett.* **2011**, *2* (24), 3006−3012.
(35) Li, S. S.; Tu, K. H.; Lin, C. C.; Chen, C. W.; Chhowalla, M. Solution-Processable Graphene Oxide as an Efficient Hole Transport Layer in Polymer Solar Cells. *ACS Nano* **2010**, *4*, 3169−3174.
(36) An, X.; Simmons, T. J.; Shah, R.; Wolfe, C.; Lewis, K. M.; Washington, M.; Nayak, S. K.; Talapatra, S.; Kar, S. Stable Aqueous Dispersion of Non-covalently Functionalized Graphene from Graphite and Their Multifunctional High-Performance Applications. *Nano Lett.* **2010**, *11*, 4295−4301.